Scientific Research Publishing

Open Journal of Civil Engineering, 2024, 14, 334-347
https://www.scirp.org/journal/ojce
ISSN Online: 2164-3172
ISSN Print: 2164-3164

Exploring the Synergy: Experimental and Theoretical Investigation of Steel and Glass Fiber Reinforced Polymer (GFRP) Reinforced Slab Incorporating Alccofine and M-Sand

Vijayalakshmi Ravichandran[1*], Ravichandran Ramanujam Srinivasan[1], Saravanan Jagadeesan[1], Prithiviraj Chidambaram[2]

[1]Department of Civil and Structural Engineering, Annamalai University, Chidambaram, India
[2]Department of Civil Engineering, SRM Madurai College for Engineering and Technology, Tamilnadu, India
Email: *ausjs5070@gmail.com, rajprithivi3@gmail.com

How to cite this paper: Vijayalakshmi, R., Ravichandran, R.S., Saravanan, J. and Prithiviraj, C. (2024) Exploring the Synergy: Experimental and Theoretical Investigation of Steel and Glass Fiber Reinforced Polymer (GFRP) Reinforced Slab Incorporating Alccofine and M-Sand. *Open Journal of Civil Engineering*, **14**, 334-347.
https://doi.org/10.4236/ojce.2024.143017

Received: June 9, 2024
Accepted: August 18, 2024
Published: August 21, 2024

Abstract

Introduction: This study investigates the Experimental and Theoretical Investigation of Steel and Glass Fiber Reinforced Polymer (GFRP) Reinforced Slab Incorporating Alccofine and M-sand. Objective: Specific objectives include evaluating the mechanical properties and structural behaviour of steel and GFRP-reinforced one-way slabs and comparing experimental and theoretical predictions. Methods: Four different mix proportions were arrived at, comprising both conventional concrete and Alccofine-based concrete. In each formulation, a combination of normal river sand and M-sand was utilized. Results: Concrete with Alccofine exhibits superior mechanical properties, while M-sand incorporation minimally affects strength but reduces reliance on natural sand. GFRP-reinforced slabs display distinct brittle behaviour with significant deflections post-cracking, contrasting steel-reinforced slabs' gradual, ductile failure. Discrepancies between experimental data and design recommendations underscore the need for guideline refinement. Conclusion: Alccofine and M-sand enhance concrete properties, but reinforcement type significantly influences slab behaviour. GFRP-reinforced slabs, though exhibiting lower values than steel, offer advantages in harsh environments, warranting further optimization.

Keywords

Fiber Reinforced Polymer, Alccofine Concrete, Structural Behaviour, Mechanical Properties, One-Way Slab, Sustainable Construction Materials,

Alternative Aggregates

1. Introduction

In the realm of civil engineering, the evolution of construction materials and techniques is an ongoing quest to enhance the durability, sustainability, and structural performance of buildings and infrastructure [1]. The integration of alternative materials in construction practices has become a pivotal avenue for researchers and practitioners alike, aiming to address the environmental impact and resource depletion associated with traditional construction materials [2] [3]. Among the myriad of alternatives, Glass Fiber Reinforced Polymer (GFRP) and Alccofine, combined with the innovative use of M-sand (manufactured sand), have emerged as promising elements in the construction paradigm [4]-[6]. This research journal embarks on a comprehensive exploration of the Experimental and Theoretical Investigation of Steel and GFRP Reinforced Slabs that incorporate M-sand and Alccofine, unravelling their potential to revolutionize contemporary construction practices.

The demand for sustainable and resilient construction materials has intensified in the face of climate change, resource scarcity, and the need for eco-friendly construction practices [7]-[9]. Steel-reinforced concrete, a ubiquitous material in construction, is not without its drawbacks, such as corrosion susceptibility and environmental concerns linked to excessive use of natural resources [10]-[12]. The incorporation of GFRP, known for its high strength-to-weight ratio, corrosion resistance, and non-conductive properties, holds promise in addressing these challenges [13]-[15]. Furthermore, the utilization of M-sand, a by-product of the crushing process in the production of concrete aggregates, is gaining traction as a sustainable alternative to traditional river sand, thereby reducing the ecological footprint of construction activities [16]-[20]. Alccofine, a supplementary cementitious material, is recognized for enhancing the strength and durability of concrete while minimizing environmental impact [21]-[26].

The primary aim of this research is to conduct a comprehensive investigation into the mechanical properties and structural behaviour of steel and GFRP reinforced slabs that incorporate M-sand and Alccofine. The study seeks to achieve the following specific objectives:

- Evaluate the compressive, tensile, and elastic modulus of the mixes.
- Assess the flexural performance of the slab reinforced with steel and GFRP.
- Comparison between the theoretical and experimental to predict the behaviour of the composite slabs.

2. Materials and Methods

Eight tests on reinforced concrete slabs were carried out in the advanced struc-

tural engineering laboratory at Annamalai University in India. The study included two types of reinforcements, namely sand-coated Glass Fiber Reinforced Polymers (GFRPs) and conventional steel reinforcement, for the purpose of comparison. The subsequent sections will furnish methodology and information on the characteristics of the various materials utilized in the research, along with other essential experimental details.

2.1. Methodology

The research methodology encompasses a multifaceted approach, combining experimental investigations and theoretical modelling. Laboratory experiments will be conducted to assess the material properties, mechanical properties, and behaviour steel and GFRP reinforced slabs comprising M-sand and Alccofine. These experiments will involve the fabrication of test specimens, including both traditional steel-reinforced slabs and those incorporating GFRP. Various tests, such as compressive strength, tensile strength, elastic modulus, flexural behaviour, load-deflection, crack propagation, failure mode; strain behaviour will be conducted according to relevant international standards. Additionally, theoretical investigations are carried out to predict the behaviour of the composite slabs to enhance the understanding of the structural response and performance of the slabs.

2.2. Test Materials

2.2.1. Reinforcement

The materials employed in the experimental program are outlined in Table 1. The one-way spanning slab specimens were reinforced longitudinally with either 1) GFRP bars coated with sand, having a 12 mm diameter, or 2) 12 mm diameter steel bars. In all instances, 8 mm steel bars were utilized in the transversal direction. The mechanical characteristics of each reinforcement type utilized in the experimental campaign were determined through tensile testing. Table 1 provides key characteristic properties, including elastic modulus (E), ultimate tensile strength (fu), and yield strength (fy) for the steel bars. Notably, no yield strength values are presented for the GFRP bars, as these materials lack a yield point. **Figure 1** displays an image of the steel and GFRPs employed in the present investigation.

Table 1. Properties of reinforcements.

Rebar	Tensile Strength (MPa)	Yield Strength (MPa)	Elastic Modulus (GPa)	Poisson Ratio
Sand Coated GFRP	290	-	62.3	0.22
Steel Fe 500	640	500	200	0.3

2.2.2. Concrete

Four concrete formulations were created, comprising both conventional con-

crete and Alccofine-based concrete. In each formulation, a combination of normal river sand and M-sand was utilized. The mix proportions and concrete

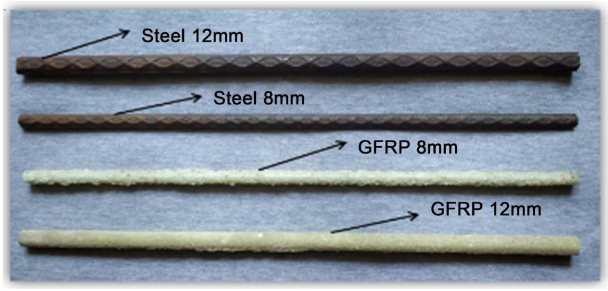

Figure 1. Reinforcements.

properties are detailed in **Table 2**. The formulations were labelled according to the materials incorporated, with "C" denoting Cement, "RS" for River Sand, "A" for Alccofine, and "MS" for M-Sand.

Table 2. Mix proportions and mechanical properties.

Description	CRS	CMS	ARS	AMS
Cement kg/m^3	348.32	348.32	296.07	296.07
Alccofine kg/m^3	-	-	52.24	52.24
River sand kg/m^3	727.15	-	727.15	-
M-sand kg/m^3	-	759.34	-	759.34
Coarse aggregate kg/m^3	1204.48	1204.48	1204.48	1204.48
Water kg/m^3	191.58	191.58	191.58	191.58
W/B ratio	0.55	0.55	0.55	0.55
Compressive strength MPa	24.03	26.34	31.97	37.02
Flexural strength MPa	3.31	3.49	3.71	3.96
Young's modulus GPa	23.72	25.84	31.56	36.83

2.3. Description of Tested Slabs

The test program included the examination of a total of eight one-way reinforced concrete slabs, as outlined in **Table 3**. These slabs were divided into four groups based on their reinforcement and binder content. Groups 1 and 2 comprised conventional concrete with steel and GFRP reinforcement, while Groups 3 and 4 consisted of Alccofine-based concrete with the same types of reinforcement. Each group featured two slabs with either river sand or M-sand. A reference system was employed to label each specimen, where the initial part of the name indicated the type of concrete (*i.e.*, Conventional Cement Concrete (C), Alccofine-based Concrete (A), River Sand (RS), and M-sand (MS)), followed by the type of reinforcement (*i.e.*, Steel Reinforcement (S) and GFRP (G)).

2.4. Preparation of Test Specimen

The slabs, with dimensions of 2000 mm in length, 600 mm in width, and 125 mm in thickness, utilize 12 mm diameter bars spaced at 280 mm c/c as the primary reinforcement, and 8 mm diameter bars spaced at 300 mm c/c as distribution reinforcement. A bottom concrete cover of 20 mm is applied. Figure 2 & Figure 3 illustrate the cross-sectional view and reinforcement arrangements of the RC slab. Before casting, strain gauges were affixed to the central longitudinal steel bar using a strong adhesive. These gauges were additionally coated with a thin resin for protection against moisture and damage. The slabs were cast using the mix proportions specified in Table 2, with concrete mixing carried out manually as depicted in Figure 4. Following casting, the specimens underwent a curing period of approximately 28 days. After this curing period, the slabs were cleaned, whitewashed, marked for support and loading, and subsequently relocated to the test floor.

Table 3. Slab details.

Specimen Group	Slab ID	Longitudinal Bar		ρ%	$\rho/\rho b$	Predicted Mode of Failure
		Steel	GFRP			
Group I	CRS-S	3#12 mm	-	0.4	0.022	Yield
	CMS-S	3#12 mm	-	0.4	0.024	Yield
Group II	CRS-G	-	3#12 mm	0.4	0.373	Rupture of rebar
	CMS-G	-	3#12 mm	0.4	0.35	Rupture of rebar
Group III	ARS-S	3#12 mm	-	0.4	0.029	Yield
	AMS-S	3#12 mm	-	0.4	0.034	Yield
Group IV	ARS-G	-	3#12 mm	0.4	0.299	Rupture of rebar
	AMS-G	-	3#12 mm	0.4	0.271	Rupture of rebar

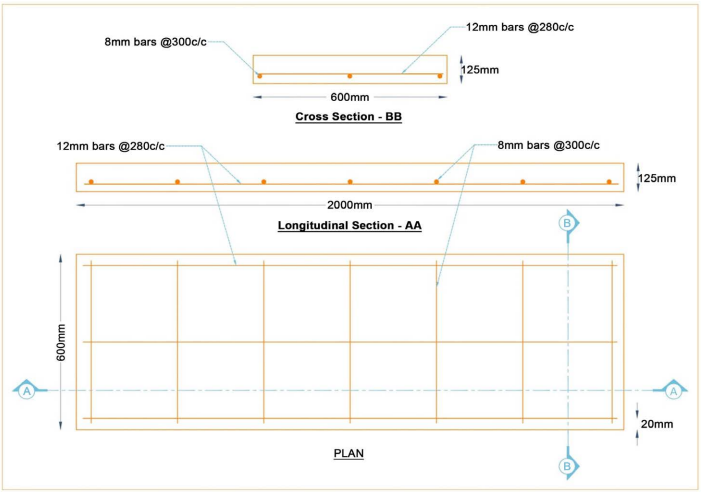

Figure 2. Plan and cross-sectional view of one-way RC slab.

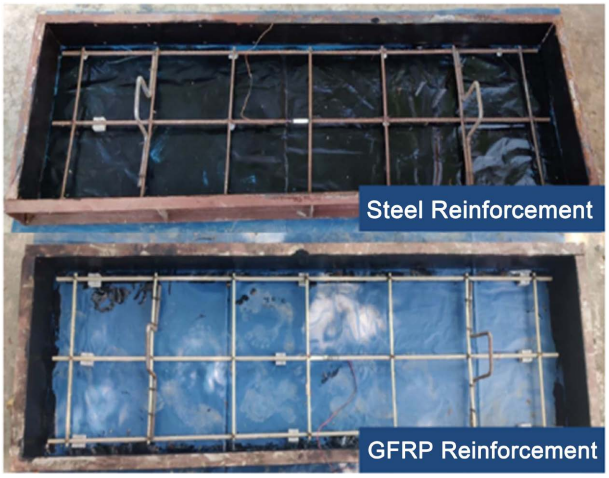

Figure 3. Reinforcement arrangements.

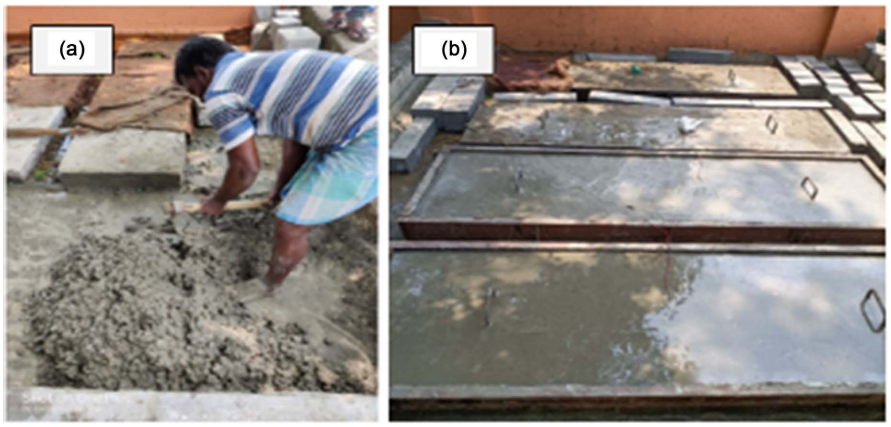

Figure 4. Casting of specimens (a) manual mixing (b) finished surface of specimen.

Test Setup

A 50-tonne capacity load frame is employed to test slab specimens, with support provided at one end through a roller and at the other end through a hinge. The slabs undergo two-point loading using a line load system facilitated by spreader beams. To prevent local effects, thick rubber or neoprene pads are placed beneath the spreader beams. The support end levels of the slabs are meticulously maintained using spirit levels. Hydraulic jacks with a manual capacity of 250 kN are utilized to apply static loads, monitored by a proving ring. Deformations in the slabs are gauged using dial gauges, strain gauges, and demec gauges. External surface strain gauges are affixed to the bottom surface of the slabs. Dial gauges are positioned at one-third distance from the supports. Demec gauges, employed for strain measurement, necessitate a standard gauge distance, achieved by affixing brass pellets at known distances at the top, center, and bottom. The load is incrementally increased by 1 kN until slab failure occurs. Crack widths at the ultimate condition are measured using a crack width detection microscope. The experimental setup is illustrated in **Figure 5**.

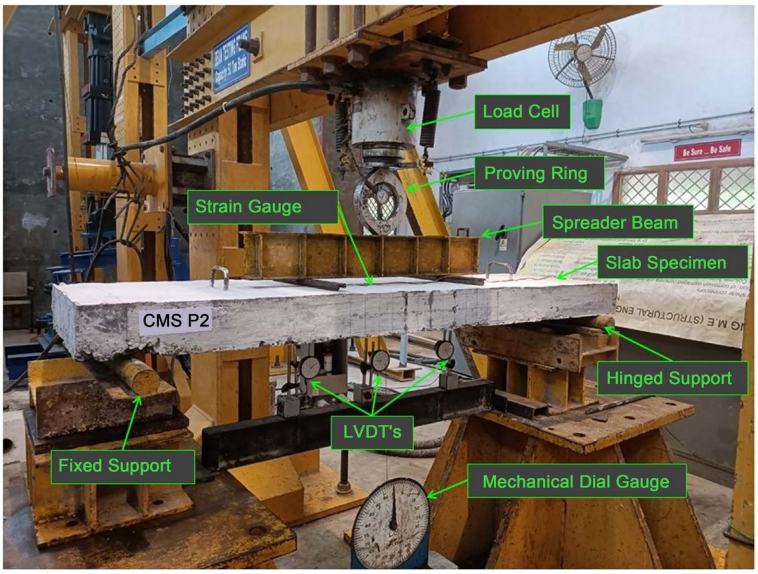

Figure 5. Experimental test setup.

3. Result and Discussion

3.1. Flexural Behaviour

In general, the slabs reinforced with steel and GFRP bars displayed a linear response before cracking occurred, followed by the sudden emergence of wide and deep cracks, accompanied by substantial deflections in GFRP reinforced slabs. The initiation and propagation of cracks in steel-reinforced concrete are often more gradual compared to sudden emergence and undergo significant deformation before failure shows the ductile response. The test outcomes and observed failure patterns for the slabs examined in this study are detailed in **Table 4**. **Figure 6** illustrates the deflected profile of the slabs. Notably, the slab reinforced with GFRP bars experiences a notable decrease in stiffness after the first crack initiation compared to the slab reinforced with steel reinforcements. Additionally, all slabs reinforced with GFRP demonstrate significantly broader crack widths and depths when compared to the slabs reinforced with steel. This divergence is ascribed to the lower elastic modulus of GFRP bars in contrast to steel reinforcements.

Table 4. Experimental observations.

Specimen Group	Slab ID	Load (kN)		Deflection (mm)		No. of Crack	Crack Width (mm)	Observed Mode of Failure
		First Crack	Ultimate	First Crack	Ultimate			
Group I	CRS-S	13.44	58.43	1.08	48.32	15	0.34	Ductile
	CMS-S	14.77	59.07	1.10	49.08	14	0.34	Ductile
Group II	CRS-G	12.30	50.02	0.82	38.68	4	3.28	FRP rupture
	CMS-G	12.50	50.38	0.85	41.21	3	2.53	FRP rupture

Continued

Group III	ARS-S	14.26	59.40	1.12	50.64	15	0.29	Ductile
	AMS-S	15.17	60.68	1.23	49.94	17	0.31	Ductile
Group IV	ARS-G	12.52	51.09	0.86	39.03	3	2.56	FRP rupture
	AMS-G	12.53	51.79	0.91	39.47	5	2.52	FRP rupture

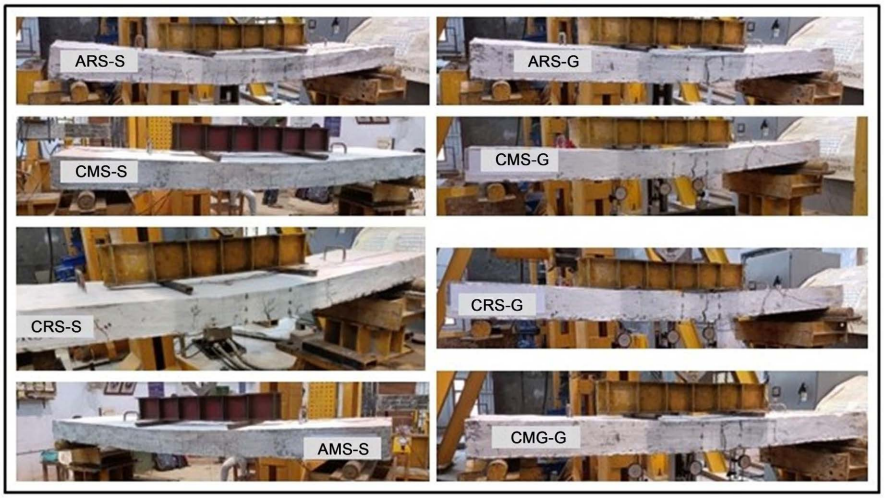

Figure 6. Deflected profiles of slabs.

3.2. Crack Propagation and Failure Modes

Figure 7 illustrates the crack propagation and crack width observed in all slabs, while Table 4 provides details on the failure modes across the slabs. In the case of slabs reinforced with steel (CRS-S, CMS-S, ARS-S, and AMS-S). The mode of failure in these instances was characterized by yielding and ductile failure. Conversely, slabs reinforced with GFRP (CRS-G, CMS-G, ARS-G, and AMS-G) exhibited a minimal number of cracks with wider crack widths. The failure mode in these slabs was brittle, resulting in the rupture of GFRP. Despite the concrete's ability to continue carrying the load, the GFRP bars experienced rupture failure, rendering them incapable of sustaining the load.

3.3. Load-Deflection Characteristics

The load-deflection behaviour of all slabs is depicted in Figure 8. The GFRP-RC slabs exhibited a bi-linear pattern, representing both pre- and post-cracking stages until eventual failure. Similar bi-linear behaviour was observed in previous studies for FRP-RC slabs subjected to static loading [27] [28]. In the case of steel-reinforced slabs, ductility is imparted to the system by the steel bars (rebars). Unlike GFRP, which tends to exhibit a more brittle failure mode, the inclusion of steel reinforcement allows for increased deformation and energy absorption before reaching failure. Consequently, the load-deflection curve of a steel-reinforced slab displays a more gradual and ductile response, lacking a

sharp transition between pre- and post-cracking behaviour. Deformation and cracking are more evenly distributed, leading to a failure that is not as abrupt or catastrophic as observed in GFRP-RC slabs.

3.4. Load-Strain Behaviour for Concrete and Reinforcement

The diagram in Figure 9 illustrates the load-strain characteristics of both reinforcement and concrete. At the moment of cracking, a sudden decline in strain was observed, followed by a rapid increase in average post-cracking strain for GFRP reinforcement within the strain range of 0 to 4. In contrast, steel reinforcement (within the strain range of 0 to 2) exhibited a slight deviation at the cracking point and a gradual post-cracking strain increase. This behaviour was observed to be influenced by the type of reinforcement material used. It was noted that the concrete strength had a negligible impact on the strain in both steel and GFRP reinforcement bars. In the case of concrete, the strain values across all slabs were nearly identical, ranging from 0 to 2.5. The lack of significant differences in strain values is attributed to the fact that slab failures occurred only under reinforcement conditions (tension failure), and the concrete strain values did not reach the ultimate strain.

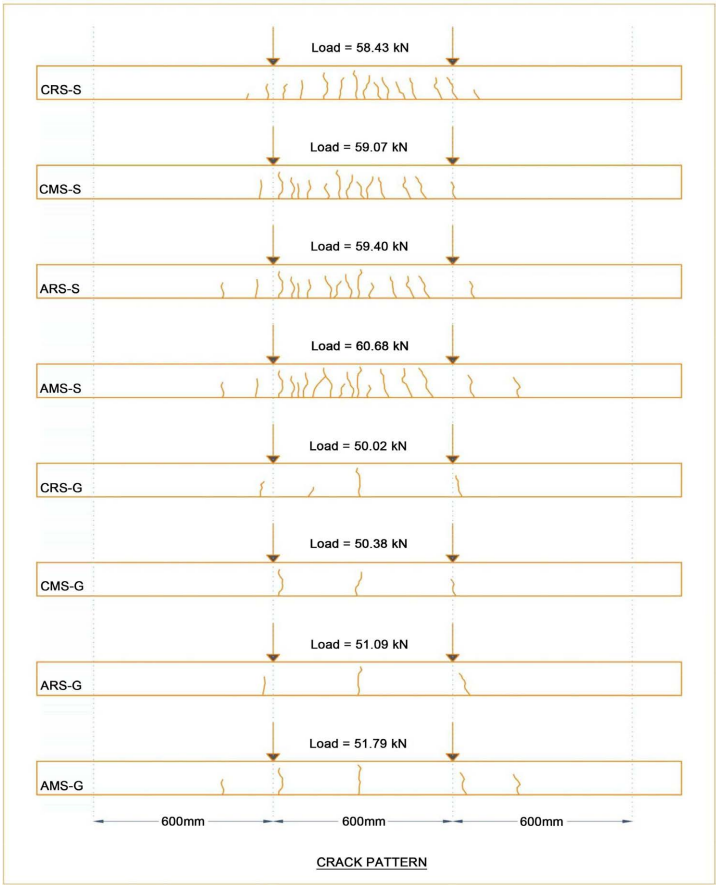

Figure 7. Crack patterns of slabs.

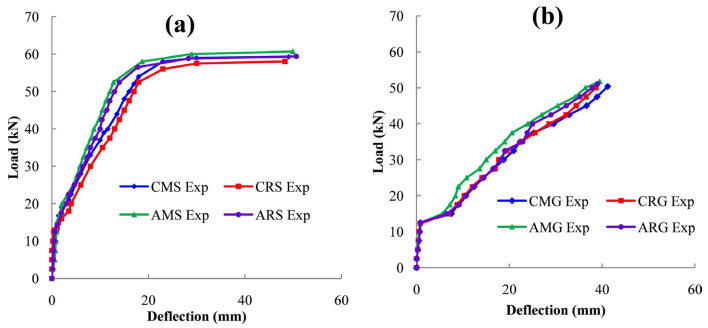

Figure 8. Load deflection curves (a) steel RC slabs & (b) GFRP RC slabs.

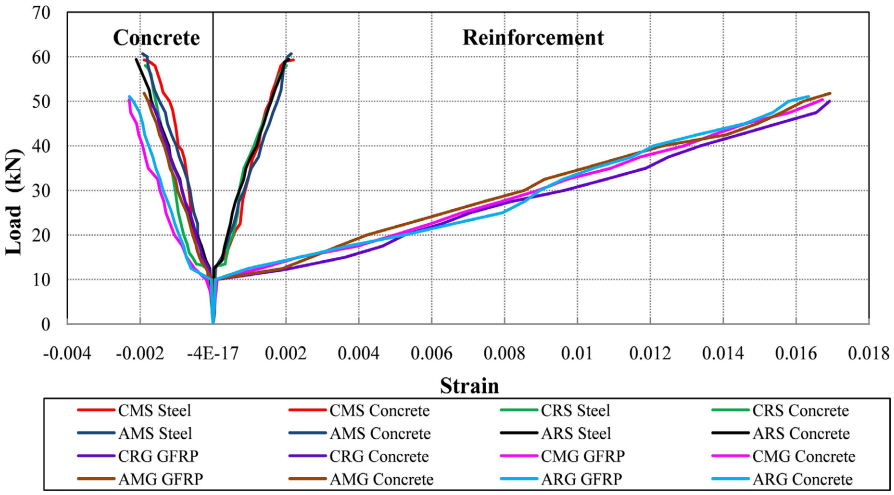

Figure 9. Load strain behaviour.

3.5. Experimental Results versus Code-Recommendations

The study involved a comparison between experimental test data and design recommendations [13] [29] focusing on failure mode, ultimate load, and deflection. The calculations for reinforcement ratios, maximum loads, and midspan deflections at maximum loads were derived from preliminary material testing data. **Table 5** displays the comparison of maximum loads and midspan deflections, presenting both experimental and code predictions, and showcasing the percentage difference. Values less than one indicate under-prediction by the design codes, while values greater than one suggest over-prediction. For example, the Slab CRS-S has load and deflection of 1.24 and 1.19 which is overpredicted by the code recommendation. Notably, slabs with a reinforcement ratio of 0.4 (less than 1) failed due to GFRP bar rupture and exhibited ductility for steel bars. **Figure 10** illustrates the load-deflection behaviour, comparing experimental and predicted outcomes.

For the analysis of cracked GFRP reinforced slabs, ACI 440 specifies the use of the effective moment of inertia (Ie) in Equation (1), incorporating an integration factor "γ" based on loading and boundary conditions. Equation (2) accounts for the integration factor in the case of four-point loading, considering the stiffness

Table 5. Comparison of experimental vs. theoretical.

Slab ID	ρ/ρb	Experimental		Theoretical		Exp/Theo	
		Load (kN)	Deflection (mm)	Load (kN)	Deflection (mm)	Load (kN)	Deflection (mm)
CRS-S	0.022	58.43	48.32	47.00	40.66	1.24	1.19
CMS-S	0.024	59.07	49.08	47.50	39.66	1.24	1.24
CRS-G	0.373	50.02	38.68	57.34	32.20	0.87	1.20
CMS-G	0.35	50.38	41.21	57.54	33.36	0.88	1.24
ARS-S	0.029	59.40	50.64	49.00	45.62	1.21	1.11
AMS-S	0.034	60.68	49.94	50.00	44.67	1.21	1.12
ARS-G	0.299	51.09	39.03	58.34	33.32	0.88	1.17
AMS-G	0.271	51.79	39.47	58.64	32.12	0.88	1.23

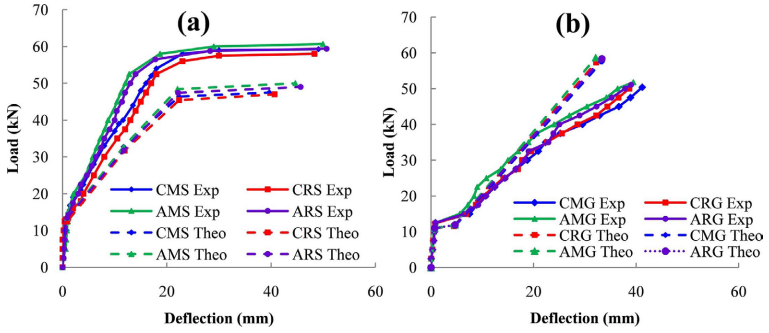

Figure 10. Comparison load deflection curves of experimental vs. theoreti-cal (a) steel RC slabs & (b) GFRP RC slabs.

along the GFRP reinforced slabs. Additionally, ACI 440 provides Equation (3) to calculate deflections and cracking for four-point loading.

$$I_e = \frac{I_{cr}}{1-\gamma\left(\frac{M_{cr}}{M_a}\right)^2\left[1-\frac{I_{cr}}{I_g}\right]} \le I_g \tag{1}$$

$$\gamma = 1.72 - 0.72\frac{M_{cr}}{M_a} \tag{2}$$

$$\Delta = \frac{23PL^3}{1296E_cI_e} \tag{3}$$

4. Conclusion

Concrete with Alccofine (ARS & AMS) shows superior mechanical properties compared to traditional concrete (CRS & CMS). Incorporating M-sand may not significantly affect strength but can reduce the need for natural river sand. GFRP-reinforced slabs (CRS-G, CMS-G, ARS-G & AMS-G) exhibit distinct behaviour: abrupt crack emergence, significant deflections, and reduced stiffness

post-cracking compared to steel-reinforced slabs, reflecting GFRP's lower elastic modulus. Steel-reinforced slabs (CRS-S, CMS-S, ARS-S & AMS-S) display yielding and ductile failure, with crack propagation mainly in the tension zone. In contrast, GFRP-reinforced slabs experience brittle failure with GFRP bar rupture, despite concrete's load capacity. Steel-reinforced slabs show gradual, ductile load-deflection behaviour due to steel reinforcement, offering increased deformation and energy absorption before failure, providing a more resilient structural response. The study highlights differing load-strain behaviours between GFRP and steel reinforcement, with GFRP showing sudden decline and rapid post-cracking strain increase, contrasting with steel's gradual deviation and strain increase. Concrete strength minimally affects reinforcement strain. Significant disparities exist between experimental data and FRP design recommendations, with over-prediction for steel-reinforced slabs and under-prediction for GFRP-reinforced slabs, emphasizing the need for refining design guidelines. Considering reinforcement ratios is crucial, as slabs with lower ratios experience GFRP bar rupture and demonstrate distinct ductility characteristics for steel bars. In summary, Alccofine and M-Sand enhance concrete properties, but reinforcement plays a dominant role in RC-Slabs. GFRP RC slabs, despite lower values compared to steel RC slabs, are more desirable in harsh environments and coastal areas, with the potential for further refinement. Moreover, adding additional GFRP reinforcement with a reduction in spacing could increase the strength and performance of the slab compared to steel-reinforced slabs. Therefore, further investigation is required to explore this potential enhancement.

Availability of Data and Materials

The data supporting the findings of this paper are available within the paper.

Conflicts of Interest

The authors declare no conflict of interest, financial or otherwise.

References

[1] Kiani Mavi, R., Gengatharen, D., Kiani Mavi, N., Hughes, R., Campbell, A. and Yates, R. (2021) Sustainability in Construction Projects: A Systematic Literature Review. *Sustainability*, **13**, Article No. 1932. https://doi.org/10.3390/su13041932

[2] Nilimaa, J. (2023) Smart Materials and Technologies for Sustainable Concrete Construction. *Developments in the Built Environment*, **15**, Article 100177. https://doi.org/10.1016/j.dibe.2023.100177

[3] Prithiviraj, C., Swaminathan, P., Kumar, D.R., Murali, G. and Vatin, N.I. (2022) Fresh and Hardened Properties of Self-Compacting Concrete Comprising a Copper Slag. *Buildings*, **12**, Article No. 965. https://doi.org/10.3390/buildings12070965

[4] Elavenil, S. and Vijaya, B. (2013) Manufactured Sand, a Solution and an Alternative to River Sand and in Concrete Manufacturing. *International Journal of Civil Engineering Research and Development*, **3**, 1-7.

[5] Prithiviraj, C. and Saravanan, J. (2021) Flexural Performance of Alccofine-Based Self-Compacting Concrete Reinforced with Steel and GFRP Bars. *International Transaction Journal of Engineering, Management, & Applied Sciences & Technologies*, **12**, 1-12.

[6] Al-Furjan, M.S.H., Shan, L., Shen, X., Zarei, M.S., Hajmohammad, M.H. and Kolahchi, R. (2022) A Review on Fabrication Techniques and Tensile Properties of Glass, Carbon, and Kevlar Fiber Reinforced Rolymer Composites. *Journal of Materials Research and Technology*, **19**, 2930-2959. https://doi.org/10.1016/j.jmrt.2022.06.008

[7] UNEP (2021) A Practical Guide to Climate-Resilient Buildings and Communities. https://www.unep.org/gan/resources/toolkits-manuals-and-guides/practical-guide-climate-resilient-buildings-communities#:~:text=A%20Practical%20Guide%20to%20Climate%2Dresilient%20Buildings%20%26%20Communities%20offers%20construction,in%20hot%20and%20humid%20climates

[8] Castaño-Rosa, R., Pelsmakers, S., Järventausta, H., Poutanen, J., Tähtinen, L., Rashidfarokhi, A., *et al.* (2022) Resilience in the Built Environment: Key Characteristics for Solutions to Multiple Crises. *Sustainable Cities and Society*, **87**, Article 104259. https://doi.org/10.1016/j.scs.2022.104259

[9] Mullan, M. (2018) Climate-Resilient Infrastructure. Policy Perspectives. *OECD Environment Policy Papers*, **14**, 1-46.

[10] American Concrete Institute (2014) ACI Committee 318, ACI 318-14: Building Code Requirements for Reinforced Concrete. Vol. 552, pp. 1-524.

[11] Angst, U.M. (2018) Challenges and Opportunities in Corrosion of Steel in Concrete. *Materials and Structures*, **51**, Article No. 4. https://doi.org/10.1617/s11527-017-1131-6

[12] Belabid, A., Elminor, H. and Akhzouz, H. (2022) The Concept of Hybrid Construction Technology: State of the Art and Future Prospects. *Future Cities and Environment*, **8**, 1-16. https://doi.org/10.5334/fce.159

[13] American Concrete Institute (2015) ACI Committee 440.1R-15, Guide for the Design and Construction of Structural Concrete Reinforced with Firber-Reinforced Polymer (FRP) Bars (ACI440.1R-15). Vol. 22, pp. 1-88.

[14] Mugahed Amran, Y.H., Alyousef, R., Rashid, R.S.M., Alabduljabbar, H. and Hung, C. (2018) Properties and Applications of FRP in Strengthening RC Structures: A Review. *Structures*, **16**, 208-238. https://doi.org/10.1016/j.istruc.2018.09.008

[15] El-Hassan, H. and El Maaddawy, T. (2019) Microstructure Characteristics of GFRP Reinforcing Bars in Harsh Environment. *Advances in Materials Science and Engineering*, **2019**, 1-19. https://doi.org/10.1155/2019/8053843

[16] Sudha, C., Ravichandran, P.T., Krishnan, K.D., Rajkumar, P.R.K. and Anand, A. (2016) Study on Mechanical Properties of High Performance Concrete Using M-Sand. *Indian Journal of Science and Technology*, **9**, 1-6. https://doi.org/10.17485/ijst/2016/v9i5/87262

[17] Anh, L.H., Mihai, F., Belousova, A., Kucera, R., Oswald, K., Riedel, W., *et al.* (2023) Life Cycle Assessment of River Sand and Aggregates Alternatives in Concrete. *Materials*, **16**, Article No. 2064. https://doi.org/10.3390/ma16052064

[18] Suriya, D., Chandar, S.P. and Ravichandran, P.T. (2023) Impact of M-Sand on Rheological, Mechanical, and Microstructural Properties of Self-Compacting Concrete. *Buildings*, **13**, Article No. 1126. https://doi.org/10.3390/buildings13051126

[19] Srivastava, A. and Singh, S.K. (2020) Utilization of Alternative Sand for Preparation of Sustainable Mortar: A Review. *Journal of Cleaner Production*, **253**, Article 119706. https://doi.org/10.1016/j.jclepro.2019.119706

[20] Kesavakannan, M. and Vasudevan, R. (2023) Structural Performance of Hybrid FRP Laminates on Concrete Beams Made with Manufactured Sand. *Matéria* (*Rio de Janeiro*), **28**, e20230186. https://doi.org/10.1590/1517-7076-rmat-2023-0186

[21] Chidambaram, P. and Jagadeesan, S. (2022) Characteristics of Self-Compacting Concrete with Different Size of Coarse Aggregates and Alccofine. *Trends in Sciences*, **19**, Article No. 3042. https://doi.org/10.48048/tis.2022.3042

[22] Prithiviraj, C., Saravanan, J., Ramesh Kumar, D., Murali, G., Vatin, N.I. and Swaminathan, P. (2022) Assessment of Strength and Durability Properties of Self-Compacting Concrete Comprising Alccofine. *Sustainability*, **14**, Article No. 5895. https://doi.org/10.3390/su14105895

[23] Prithiviraj, C. and Saravanan, J. (2020) Influence of W/B Ratio and Chemical Admixture on Fresh and Hardened Properties of Self Compacting Concrete Using Alccofine. *Journal of Xidian University*, **14**, 4906-4915.

[24] Balamuralikrishnan, R. and Saravanan, J. (2021) Effect of Addition of Alccofine on the Compressive Strength of Cement Mortar Cubes. *Emerging Science Journal*, **5**, 155-170. https://doi.org/10.28991/esj-2021-01265

[25] Sagar, B. and Sivakumar, M.V.N. (2020) An Experimental and Analytical Study on Alccofine Based High Strength Concrete. *International Journal of Engineering*, **33**, 530-538.

[26] Balamuralikrishnan, R. and Saravanan, J. (2019) Effect of Alccofine and GGBS Addition on the Durability of Concrete. *Civil Engineering Journal*, **5**, 1273-1288. https://doi.org/10.28991/cej-2019-03091331

[27] Michaluk, C.R., Rizkalla, S.H., Tadros, G. and Benmokrane, B. (1998) Flexural Behavior of One-Way Concrete Slabs Reinforced by Fiber Reinforced Plastic Reinforcements. *ACI Structural Journal*, **95**, 353-365.

[28] Adam, M.A., Erfan, A.M., Habib, F.A. and El-Sayed, T.A. (2021) Structural Behavior of High-Strength Concrete Slabs Reinforced with GFRP Bars. *Polymers*, **13**, Article No. 2997. https://doi.org/10.3390/polym13172997

[29] Bureau of Indian Standard (2000) IS 456, Plain and Reinforced Concrete. Vol. 4, 1-114.

List of Abbreviations

ACI = American Concrete Institute

GFRP = Glass Fiber Reinforced Polymer

RC = Reinforced Concrete